

Disorder-induced topological superconductivity in a spherical quantum-Hall–superconductor hybrid

Koji Kudo, Ryota Nakai, and Kentaro Nomura
Department of Physics, Kyushu University, Fukuoka 819-0395, Japan

Quantum-Hall–Superconductor hybrids have been predicted to exhibit various types of topological order, providing possible platforms for intrinsically fault-tolerant quantum computing. In this paper, we develop a formulation to construct this hybrid system on a sphere, a useful geometry for identifying topologically ordered states due to its compact and contractible nature. As a preliminary step using this framework, we investigate disorder effects on the Rashba-coupled quantum Hall system combined with the type-II superconductor. By diagonalizing the BdG Hamiltonian projected into a Rashba-coupled Landau level, we demonstrate the emergence of a topological superconducting phase resulting from disorders and proximity-induced pairing. Distinctive gapless modes appear in the real-space entanglement spectrum, which is consistent with topological superconductivity.

I. INTRODUCTION

The topology of the many-body configuration space determines possible quantum statistics of particles [1]. The fundamental group of the configuration space is the symmetry group in three or higher dimensions while the braid group in two dimensions, allowing exotic particles beyond bosons and fermions, namely anyons [2]. The emergence of anyonic quasiparticles is a defining feature of topological order [3], which has revealed a new aspect of phases of matter beyond the scope of Landau’s theory. Typical examples of topologically ordered states are the fractional quantum Hall (FQH) effect [4–6], quantum spin liquids [7–10], and $p + ip$ superconductors (SCs) [11, 12]. Recent progress in experiments for anyons has been made, for example, through measurements of the half-integer quantized thermal Hall conductivity in the Kitaev materials [13–15] and detections of the fractional statistics via directly braiding the FQH quasiparticles [16–18]. Creating, manipulating, and reading non-Abelian anyons are basic elements for topological quantum computing [19–21], which has been an ultimate goal in condensed matter physics.

A key strategy for generating non-Abelian anyon platforms has involved designing topological materials. Hybridizing well-understood ingredients, even if they are not inherently topological, has proved to be a valuable tool in this process, leveraging their interplay to introduce topological order. For instance, hybridization with s -wave non-topological SCs induces superconducting proximity effects, leading to Majorana modes on surfaces of strong topological insulators [22, 23], spin-orbit coupled semiconductors [24–27], quantum anomalous Hall systems [28], and integer quantum Hall (IQH) systems [29–31]. Recent efforts have been directed towards exploring hybrid quantum-Hall–SC (QH-SC) systems that host much more exotic particles such as parafermions [32–41] and Fibonacci anyons [42–46] (The so-called QH superconductivity [47–67] also exhibits similar physics as the QH-SC hybrids). These developments have highlighted the potential of QH-SC hybrids for universal topological quantum computation.

In theoretical exploration of topological order, the geometry of systems is quite crucial. Particularly, boundaries introduce low-energy modes as edge states [68, 69], rendering compact surfaces suitable for investigating bulk properties of topologically ordered states. On a compact surface with genus $g \geq 1$, the one-dimensional unitary representation of the braid group is absent. Consequently, states on such surfaces must be degenerate to form a multi-component structure [70–75], referred to as topological degeneracy [76, 77]. This phenomenon, while intriguing and closely related to topological nature of anyons, can pose technical challenges in numerical studies. Indeed, the spherical geometry [78] with $g = 0$ has been commonly used in the FQH physics.

This background motivates us to develop a formulation to construct a hybrid QH-SC system with the spherical

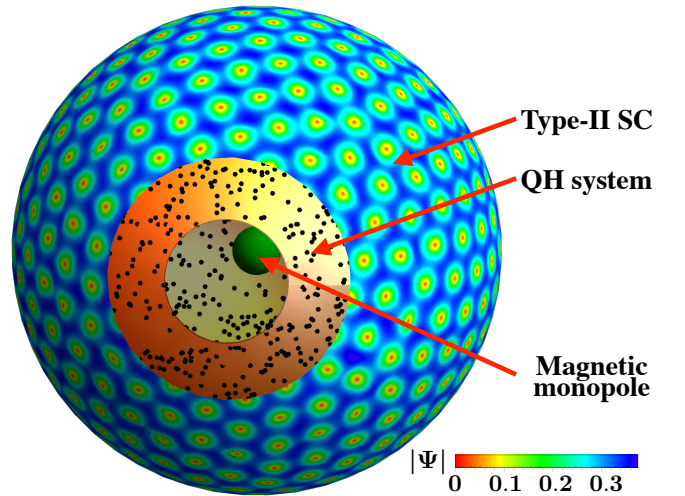


FIG. 1. QH-SC hybrid on a sphere. The outer (inner) surface represents the type-II SC (QH system). The color of the outer surface indicates the order parameter $|\Psi|$ at $2\bar{Q} = 450$. We normalize Ψ as $\int d\bar{\Omega} |\Psi|^2 = 1$ for simplicity. The black dots in the inner surface depict impurities, with a total count of 4500. The order (outer or inner) of each system is not significant. The green sphere at the center is the magnetic monopole.

geometry. As a preliminary step, we consider the Rashba-coupled IQH system combined with the type-II SCs, motivated by Refs. 30 and 31. In addition, we incorporate random distributions of δ -function impurities. Figure 1 visually represents our model. The type-II SC is chosen because of the strong magnetic field required for the QH system. Our numerical studies demonstrate that the interplay between disorders and proximity-induced pairing results in a topological superconducting phase associated with the half-integer Chern number [equivalently the unit Bogoliubov–de Gennes (BdG) Chern number]. We identify this phase by detecting gap-closing lines. The entanglement spectrum reveals distinctive gapless modes, providing further evidence for topological superconductivity.

The paper is organized as follows. In Sec. II, we review two components in our hybrid system on a sphere: the Rashba-coupled QH system and a model type-II SC. In Sec. III, we construct the hybrid QH-SC system. Section IV presents numerical results, and the paper concludes in Sec. V.

II. SETUP FOR THE SPHERICAL GEOMETRY

A. Rashba-coupled Landau level

We begin by considering the Rashba-coupled Landau level (LL) structure. The single-particle Hamiltonian reads $H_1 = \vec{\pi}^2/2m - \alpha_R(\vec{\sigma} \times \vec{\pi})$, where $\vec{\pi}$ is the canonical momentum, $\vec{\sigma}$ is the Pauli matrices, and α_R is the Rashba coupling strength. In the planar geometry, this reduces to [30, 31, 79–83]

$$H_1 = \hbar\omega_c \begin{pmatrix} a^\dagger a + \frac{1}{2} & -ig_R a \\ ig_R a^\dagger & a^\dagger a + \frac{1}{2} \end{pmatrix}, \quad (1)$$

where $\omega_c = eB/mc$ is the cyclotron frequency and $g_R = \sqrt{2}\alpha_R/l_B\omega_c$ with l_B the magnetic strength. The ladder operator is defined by $a^\dagger = (\pi_x + i\pi_y)l_B/\sqrt{2}\hbar$. Within the subspace,

$$\Phi_{nm} = (|n-1, m\rangle, |n, m\rangle) \text{ with } n \geq 1, \quad (2)$$

where $|n, m\rangle$ is the eigenstate of angular momentum $\hbar m$ in the n th LL without spin-orbit coupling, the Hamiltonian H_1 is block-diagonalized as

$$\Phi_{nm}^\dagger H_1 \Phi_{nm} = \hbar\omega_c \begin{pmatrix} n - \frac{1}{2} & -ig_R\sqrt{n} \\ ig_R\sqrt{n} & n + \frac{1}{2} \end{pmatrix}. \quad (3)$$

Its eigenvalues and eigenvectors are

$$\begin{aligned} \epsilon_{n\pm} &= \hbar\omega_c \left(n \pm \sqrt{1/4 + g_R^2 n} \right), \\ \vec{v}_{n\pm} &= \left(i/2 \mp i\sqrt{g_R^2 n + 1/4} \right) / \mathcal{N}, \end{aligned} \quad (4)$$

where \mathcal{N} is a normalization factor. In addition, the unpaired state $(0, |0, m\rangle)$ is an eigenstate of H_1 with energy

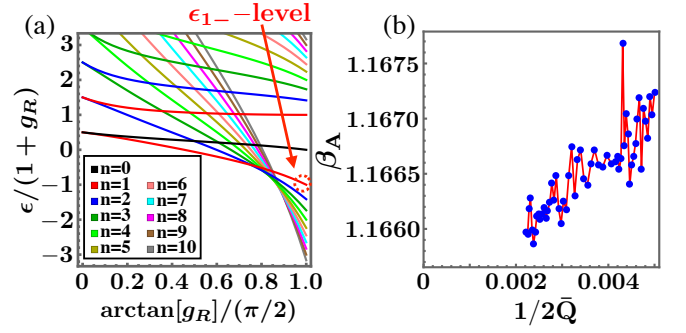


FIG. 2. (a) Rashba-coupled LLs ϵ_0 and $\epsilon_{n\pm}$ with $n \leq 10$. (b) Abrikosov factor β_A at various $2\bar{Q}$'s.

$\epsilon_0 = \hbar\omega_c/2$. In the limit $g_R \rightarrow \infty$, H_1 reduces to the Hamiltonian of massless Dirac fermions.

Figure 2(a) shows the single-particle energy. To observe the evolution for $g_R \in [0, \infty)$, we scale the energy by $1 + g_R$ and plot it as a function of $\arctan(g_R)$. At $g_R \sim 0$, the energy is quantized in increments of n while in increments of \sqrt{n} at $g_R \sim \infty$. In the next section, we will focus on the Rashba-coupled LL with ϵ_{1-} , referred to as ϵ_{1-} -level. This is the lowest energy level for $0 < g_R < \sqrt{6}$ and becomes the “ $n = -1$ LL” of the two-dimensional Dirac Hamiltonian [84] as g_R approaches infinity.

In the following, we consider Haldane’s spherical geometry [78], where N particles move on the surface under a radial magnetic field. The total radial flux is $2Q\phi_0$, where $\phi_0 = hc/e$ is the flux quantum and $2Q$ is an integer. In the spinless problem without spin-orbit coupling, single-particle states are labeled by the orbital angular momentum l and its z -component m because of rotational symmetry. Their possible values are $l = |Q|, |Q| + 1, \dots$ and $m = -l, -l + 1, \dots, l$. The $2l + 1$ states with $l = |Q| + n$ corresponds to the n th LL. The eigenstates are the monopole harmonics $Y_{Qlm}(\vec{\Omega})$ [85, 86], where $\vec{\Omega}$ represents the angular coordinates θ and ϕ .

Spin-orbit coupling is not straightforward to apply as it mixes different LLs having different degrees of degeneracy on a sphere. The same issue also arises, e.g. in the QH physics in graphene [87–92]. Fortunately, because of the non-flat geometry, relativistic electrons on a Haldane’s sphere with physical fluxes Q are subject to different magnetic fluxes $Q_{\pm} = Q \pm 1/2$ depending on the spin orientation [93–96]. As a result, n th LL with Q_+ and $(n + 1)$ th LL with Q_- have the same degree of degeneracy. Based on this solution, we use the following basis, instead of Eq. (2), for the spherical geometry:

$$\Phi_{Qnm} = (Y_{Q_+, Q_+ + n, m}, Y_{Q_-, Q_+ + n, m}). \quad (5)$$

The labels n, m represent the Landau index and the angular momentum.

B. Abrikosov vortex lattice

We now review a model type-II superconductor on a sphere [97, 98] to calculate the superconducting order parameter, which we will use to construct the proximity-induced pairing amplitude in our hybrid system below. Here we consider a clean system with a magnetic field slightly smaller than the upper critical field H_{c2} . A magnetic monopole is placed at the center of the sphere in the same fashion as above. For clarity, we mark quantities for Cooper pairs by a bar; superconducting flux quantum $\bar{\phi}_0 = hc/\bar{e}$ with $\bar{e} = 2e$ and the total flux $2\bar{Q}\bar{\phi}_0$ (equivalently, $\bar{Q} = 2Q$).

To identify the superconducting order parameter, we consider the GL free energy $\mathcal{F}[\Psi] = \int d\vec{\Omega} f[\Psi]$ with

$$f[\Psi] = -a|\Psi|^2 + \frac{b}{2}|\Psi|^4 + \frac{1}{2m} \left| \left(\frac{\hbar}{i} \vec{\nabla} + \frac{\bar{e}}{c} \vec{A} \right) \Psi \right|^2 + \frac{|\vec{B}|^2}{8\pi}, \quad (6)$$

where a, b are phenomenological parameters ($a, b > 0$). We now demonstrate that Ψ minimizing \mathcal{F} does not depend on a and b except the overall amplitude. Close to the upper critical field, the order parameter lies in the lowest LL of Cooper pairs as

$$\Psi(\vec{\Omega}) = \sum_{\bar{m}=\bar{Q}}^{\bar{Q}} u_{\bar{m}} Y_{\bar{Q}\bar{Q}\bar{m}}(\vec{\Omega}), \quad (7)$$

and one obtains

$$-a \int d\vec{\Omega} |\Psi|^2 = -a \vec{u}^\dagger \vec{u}, \quad (8)$$

$$\frac{b}{2} \int d\vec{\Omega} |\Psi|^4 = \frac{b}{2} \sum_{s=-2\bar{Q}}^{2\bar{Q}} \left| \vec{u}^T K^{(s)} \vec{u} \right|^2, \quad (9)$$

where $\vec{u} = (u_{-\bar{Q}}, u_{-\bar{Q}+1}, \dots, u_{\bar{Q}})$ and,

$$K_{ij}^{(s)} = S \begin{pmatrix} \bar{Q} & \bar{Q} & -2\bar{Q} \\ \bar{Q} & \bar{Q} & 2\bar{Q} \\ i & j & -i-j \end{pmatrix} \delta_{s,i+j}, \quad (10)$$

$$S \begin{pmatrix} Q_1 & Q_2 & Q_3 \\ l_1 & l_2 & l_3 \\ m_1 & m_2 & m_3 \end{pmatrix} \equiv \int d\vec{\Omega} Y_{Q_1 l_1 m_1} Y_{Q_2 l_2 m_2} Y_{Q_3 l_3 m_3}. \quad (11)$$

Dropping the constant, the GL free energy reduces to

$$\mathcal{F}(\vec{u}) = -ax + \frac{b}{2} \frac{\beta_A}{4\pi} x^2, \quad (12)$$

where $x = \vec{u}^\dagger \vec{u}$ and β_A is the Abrikosov factor:

$$\beta_A \equiv \frac{\langle |\Psi|^4 \rangle}{\langle |\Psi|^2 \rangle^2} = \frac{4\pi \sum_s \left| \vec{u}^T K^{(s)} \vec{u} \right|^2}{(\vec{u}^\dagger \vec{u})^2}. \quad (13)$$

Here $\langle \cdot \rangle$ represents a spatial average. Equation (13) implies that β_A is independent of $|\vec{u}|$ and also $x (= \vec{u}^\dagger \vec{u})$. The GL free energy has a peak at $x = 4\pi a/(b\beta_A) \equiv x_0$ and its value is

$$\mathcal{F}_{\text{peak}}(\vec{u}) = -\frac{2\pi a^2}{b\beta_A}. \quad (14)$$

Thus, minimizing \mathcal{F} is equivalent to minimizing β_A . Since β_A does not involve a and b , the solution of \vec{u} that minimizes \mathcal{F} does not either, apart from the norm (the norm of \vec{u} is determined by x_0).

We numerically minimize \mathcal{F} with $a = b = 1$ and calculate the Abrikosov factor β_A for various $2\bar{Q}$ in Fig. 2(b). The value of β_A with $2\bar{Q} \rightarrow \infty$ is 1.1652, determined through linear extrapolation. This is slightly larger than 1.1596 calculated on an infinite flat plane with triangular Abrikosov vortex lattices [99]. This deviation comes from the fact that a triangular lattice cannot generally cover a surface of a sphere [97]. In Fig. 1, we plot $|\Psi(\vec{\Omega})|$ on a sphere at $2\bar{Q} = 450$. The vortices basically form a triangular lattice but there are defects as well. Similar discussions can be found in the context of the famous Thomson problem [100–102] and the Wigner crystal in the QH problem [103].

We use the solution of \vec{u} to construct proximity-induced pairing amplitude in our hybrid system below. In Fig. 2(b), we minimize \mathcal{F} with M_{sample} different initial points of \vec{u} with $80 \leq M_{\text{sample}} \lesssim 400$. We then plot β_A if the lowest β_A is at least 3-fold degenerate. Here, two β_A 's are considered the same if their difference is less than 10^{-8} . The magnetic fluxes are set as $\bar{Q} = 100, 101, 102, \dots, 119$ and $120, 123, 126, \dots, 225$. (We failed to seek β_A that satisfies this criterion at some values of \bar{Q} 's.)

III. SPHERICAL HYBRID SYSTEM

Our spherical hybrid system is composed of a Rashba-coupled QH system with disorders and a type-II s -wave SC. Hybridization induces the superconducting proximity effect on the QH system. We write its total Hamiltonian as

$$\mathcal{H} = \int d\vec{\Omega} c^\dagger(\vec{\Omega}) \left[H_1(\vec{\Omega}) + H_{\text{imp}}(\vec{\Omega}) - \mu \right] c(\vec{\Omega}) + \int d\vec{\Omega} c_\uparrow^\dagger(\vec{\Omega}) \Delta(\vec{\Omega}) c_\downarrow^\dagger(\vec{\Omega}) + \text{h.c.}, \quad (15)$$

where $c_\sigma^\dagger(\vec{\Omega})$ is the creation operator for a fermion with spin σ , $c^\dagger = (c_\uparrow^\dagger, c_\downarrow^\dagger)$, μ is a chemical potential, and $\Delta(\vec{\Omega})$ is the pairing amplitude. Here, H_{imp} represents a random distribution of $2N_{\text{imp}} = 20Q$ impurities at positions $\vec{\Omega}_i$'s with the energy $\pm w$:

$$H_{\text{imp}}(\vec{\Omega}) = \sum_{i=1}^{2N_{\text{imp}}} (-1)^i w \delta^2(\vec{\Omega} - \vec{\Omega}_i). \quad (16)$$

The impurities broaden the LLs and their width is estimated to be $\Gamma = (w/R^2)\sqrt{4\rho/2\pi l_B^2}$, where $R = l_B\sqrt{Q}$ and $\rho = 2N_{\text{imp}}/4\pi R^2$, by using the self-consistent Born approximation [104]. We parameterize the strength of disorders by Γ rather than w below. The pairing amplitude $\Delta(\vec{\Omega})$ in Eq. (15) is defined by

$$\Delta(\vec{\Omega}) = C \sum_{\bar{m}=-\bar{Q}}^{\bar{Q}} u_{\bar{m}} Y_{\bar{Q}\bar{Q}\bar{m}}(\vec{\Omega}), \quad (17)$$

where C is a constant and $u_{\bar{m}}$ is the solution of the minimizing problem of the GL free energy \mathcal{F} discussed above. We parameterize the strength of the proximity effect by $\Delta_0 = \sqrt{|C|^2 \bar{u}^\dagger \bar{u}/(4\pi)}$, which corresponds to the spatial average of $\Delta(\vec{\Omega})$, i.e.,

$$\int d\vec{\Omega} |\Delta(\vec{\Omega})|^2 = 4\pi \Delta_0^2. \quad (18)$$

Hereafter, we consider the BdG Hamiltonian projected into the ϵ_{1-} -level as

$$\mathcal{H}_{\text{BdG}} = \frac{1}{2} \mathbf{f}^\dagger H_{\text{BdG}} \mathbf{f}, \quad (19)$$

$$H_{\text{BdG}} = \begin{pmatrix} h_0 & 2D \\ 2D^\dagger & -h_0^* \end{pmatrix}, \quad (20)$$

where h_0 and D are $(2Q_+ + 1) \times (2Q_+ + 1)$ matrices, $\mathbf{f}^\dagger = (f_{-Q_+}^\dagger, \dots, f_{Q_+}^\dagger, f_{-Q_+}, \dots, f_{Q_+})$, and f_m^\dagger is the creation operator of states in ϵ_{1-} -level defined by

$$f_m^\dagger = (d_{Q_+Q_+m\uparrow}^\dagger, d_{Q_+Q_+m\downarrow}^\dagger) \vec{v}_{1-}, \quad (21)$$

$$d_{Q_\pm lm\sigma}^\dagger = \int d\vec{\Omega} Y_{Q_\pm lm}(\vec{\Omega}) c_\sigma^\dagger(\vec{\Omega}). \quad (22)$$

Here, Q_\pm in Eq. (22) takes Q_+ (Q_-) with spin $\sigma = \uparrow$ (\downarrow). This projection is based on two assumptions: first, the chemical potential μ is close to ϵ_{1-} -level, and second, the Landau gap $\hbar\omega_c$ significantly exceeds both disorder and proximity effect. Let us now calculate the matrices h_0 and D , and discuss some properties of the BdG spectrum.

A. matrix h_0

The matrix h_0 is derived from the first term of \mathcal{H} in Eq. (15). Within the ϵ_{1-} -level space, we can perform the following replacement,

$$c_\sigma^\dagger(\vec{\Omega}) \rightarrow \sum_{m=l}^l Y_{Q_\pm lm}^*(\vec{\Omega}) d_{Q_\pm lm\sigma}^\dagger, \quad (23)$$

$$(d_{Q_+Q_+m\uparrow}^\dagger, d_{Q_+Q_+m\downarrow}^\dagger) \rightarrow f_m^\dagger \vec{v}_{1-}. \quad (24)$$

Then the disorder potential is expressed by

$$\int d\vec{\Omega} c^\dagger(\vec{\Omega}) H_{\text{imp}}(\vec{\Omega}) c(\vec{\Omega}) = \sum_{m,m'=-Q_+}^{Q_+} W_{mm'} f_m^\dagger f_{m'}, \quad (25)$$

where

$$\begin{aligned} W_{mm'} &= |[v_{1-}]_1|^2 W_{Q_+}(Q_+m; Q_+m') \\ &\quad + |[v_{1-}]_2|^2 W_{Q_-}(Q_+m; Q_+m'), \\ W_Q(lm; l'm') &= w(-1)^{Q-m'} \sum_{l''=l_i}^{l_f} \times \\ S \begin{pmatrix} -Q & Q & 0 \\ l & l' & l'' \\ -m & m' & m-m' \end{pmatrix} &\sum_{i=1}^{2N_{\text{imp}}} (-1)^i Y_{l'm'-m}(\vec{\Omega}_i), \end{aligned} \quad (26)$$

where $l_i = \max\{|l-l'|, |m-m'|\}$ and $l_f = l+l'$. Noting that H_1 becomes an identity matrix with a prefactor ϵ_{1-} , one gets

$$(h_0)_{mm'} = W_{mm'} + \delta_{mm'}(\epsilon_{1-} - \mu). \quad (27)$$

B. matrix D

The pairing amplitude is deformed as

$$\int d\vec{\Omega} c_\uparrow^\dagger(\vec{\Omega}) \Delta(\vec{\Omega}) c_\downarrow^\dagger(\vec{\Omega}) = \sum_{l'} \sum_{m'm'} \Delta(Q_+lm; Q_-l'm') \times d_{Q_+lm\uparrow}^\dagger d_{Q_-l'm'\downarrow}^\dagger \quad (28)$$

where

$$\begin{aligned} \Delta(Q_+lm; Q_-l'm') &= \int d\vec{\Omega} Y_{Q_+lm}^* Y_{Q_-l'm'} \Delta(\vec{\Omega}) \\ &= C u_{m+m'} (-1)^{\bar{Q}-m-m'} S \begin{pmatrix} -Q_+ & -Q_- & \bar{Q} \\ l & l' & \bar{Q} \\ -m & -m' & m+m' \end{pmatrix}. \end{aligned} \quad (29)$$

Noting the validity of the replacement $d_{Q_+lm\uparrow}^\dagger d_{Q_-l'm'\downarrow}^\dagger \rightarrow i\gamma f_m^\dagger f_{m'}$ within the ϵ_{1-} -level, where $i\gamma \equiv [v_{1-}]_1^* [v_{1-}]_2^* = -g_R/\sqrt{1+4g_R^2}$, one gets

$$D_{mm'} = i\gamma \Delta(Q_+Q_+m; Q_-Q_+m'). \quad (30)$$

One can easily show $D^T = -D$. The parameter γ is a monotonically decreasing function of g_R , with $\gamma(0) = 0$ and $\gamma(\infty) = -1/2$. This implies that the strength of spin-orbit coupling enhances the proximity-induced superconducting pairing [30, 31]. For the purpose of demonstrating topological superconductivity, we fix $g_R = 10^{10}$ in the numerical calculations below. In this regime, the Rashba-coupled system can be replaced with monolayer graphene or a surface of a three-dimensional topological insulator with magnetic fields.

C. BdG spectrum

The BdG spectrum is given by

$$H_{\text{BdG}} \begin{pmatrix} u_k \\ v_k \end{pmatrix} = E_k \begin{pmatrix} u_k \\ v_k \end{pmatrix}, \quad (31)$$

where u_k and v_k are N -dimensional vectors and $2N \equiv 4Q_+ + 2$ is the dimension of H_{BdG} . Here, we arrange the eigenvalues in ascending order as $E_{-(N-1/2)} \leq E_{-(N-1/2)+1} \leq \dots \leq E_{N-1/2}$. The particle-hole symmetry brings $E_{-k} = -E_k$ and $\begin{pmatrix} u_{-k} \\ v_{-k} \end{pmatrix} = \begin{pmatrix} v_k^* \\ u_k^* \end{pmatrix}$. Then, we have

$$\mathcal{H}_{\text{BdG}} = \frac{1}{2} \sum_{\text{all } k} E_k g_k^\dagger g_k = \sum_{k < 0} E_k g_k^\dagger g_k + \text{const}, \quad (32)$$

where

$$g_k^\dagger = g_{-k} = \mathbf{f}^\dagger \begin{pmatrix} u_k \\ v_k \end{pmatrix}. \quad (33)$$

The ground state is given by $|G\rangle = \prod_{k < 0} g_k^\dagger |0\rangle$ with $|0\rangle$ the vacuum state of electrons. We will use the following matrices,

$$\begin{aligned} u &\equiv (u_{-(N-1/2)}, \dots, u_{-1/2}), \\ v &\equiv (v_{-(N-1/2)}, \dots, v_{-1/2}), \end{aligned} \quad (34)$$

to calculate the entanglement spectrum below.

IV. NUMERICAL RESULTS

The system parameters we have not fixed yet are

$$(2Q, \Delta_0, \Gamma, \mu).$$

The main goal now is to find a topological superconducting phase by varying Δ_0/Γ and μ/Γ . For simplicity, we fix $\Gamma = 1$ and measure μ relative to ϵ_{1-} . The numerical results below are all obtained by diagonalizing \mathcal{H}_{BdG} in Eq. (19).

A. Energy gap

Figure 3(a) plots the energy gap—the energy separation around $E = 0$ in the BdG spectrum—as a function of μ and Δ_0 with $2Q = 198$, which is a “typical” value of $2Q$ as mentioned below. To visualize gap-closing points, we present its logarithm in Fig. 3(b). The subsequent analysis suggests that the centered phase with a star in the figure is a topological superconducting phase. Figure 3(c) explicitly shows the values of the gap at specific Δ_0 's, indicating that each local minimum corresponds to the gap-closing as long as $0 < \Delta_0 \lesssim 8.5$.

To clarify emergent phases, we generate Fig. 3(d) that displays local-minimum gap points. Here, we count the number of those points at each Δ_0 , denoted M , and then define Δ_{c1} (Δ_{c2}) as the transition points where M changes to 2 (1) as Δ_0 increases. In Fig. 3(d), we have $\Delta_{c1} \sim 3$ and $\Delta_{c2} \sim 8.5$. Let us now discuss each of the following four regions: (The ground state at $|\mu| \gg \Delta_0, \Gamma$ is completely occupied or unoccupied states. Associating the Chern number C , we call each of them “ $C = 1$ ” and “ $C = 0$ ” states, respectively.

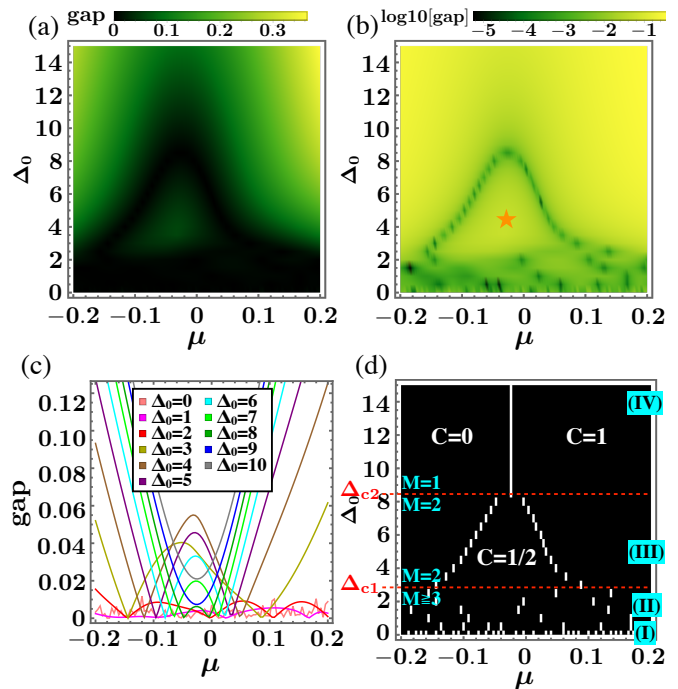


FIG. 3. (a)(b) Density plots of the energy gap and its logarithm as functions of the chemical potential μ and the pairing amplitude Δ_0 . The star in (b) indicates a topological superconducting phase. (c) Energy gap as a function of μ . (d) White points indicate the local-minimum gap. When identifying these points, we sweep μ in increments of $\delta\mu = 0.004$ at each Δ_0 . The red dashed lines represent Δ_{c1} and Δ_{c2} , representing the boundary where the number of local-minimum gap points, M , changes. There are four regions as labeled by (I)-(IV). We set $2Q = 198$ and $\Gamma = 1$ in all of the figures.

(I): $\Delta_0 = 0$: *QH plateau transition.*

A plateau transition connecting $C = 0$ and 1 phases occurs as μ is changed. Localized states induce multiple gap-closing points in Fig. 3(d).

(II): $0 < \Delta_0 < \Delta_{c1}$: *Open question.*

We have $M \geq 3$. The nature of the gap-closing points is still an open question. There are two possible scenarios: a plateau transition connecting (1) $C = 0, 1/2$ and 1 phases, or (2) $C = 0$ and 1 phases. The distinction lies in whether the intermediate state at $\mu \sim 0$ is a topological SC (see the next paragraph for more details) or a gapless state [30] arising from a network model with states carrying different Chern numbers. Determining the possibilities requires more careful calculations, which we leave for future study.

(III): $\Delta_{c1} < \Delta_0 < \Delta_{c2}$: *Emergence of $C = 1/2$ phase.*

We have $M = 2$. Given that the intermediate phase is situated between $C = 0$ and $C = 1$ phases, we expect it to be the $C = 1/2$ phase, namely a topological superconducting phase with the unit BdG Chern number. This expectation is further supported by the entanglement spectrum calculated in the next section.

(IV): $\Delta_{c_2} < \Delta_0$: *Disappearance of $C = 1/2$ phase.*

We have $M = 1$. The value of the local minimum increases as Δ_0 is increased, see Fig. 3(c). According to Ref. 30, the pairing amplitude induced from a mixed state SC contains point nodes akin to the $p+ip$ -wave pairing potential, which gives rise only two phases $C = 0$ and $C = 1$. This suggests that the observed finite minimum gap at $\Delta_0 = 9, 10$ is a finite-size effect, and therefore the line in Fig. 3(d) can be interpreted as the phase boundary dividing $C = 0$ and 1.

B. Entanglement spectrum

Now we topologically characterize the $C = 1/2$ phase. Although a typical way is to calculate the Chern number, but is fundamentally challenging in our model due to the absence of translation invariance in the spherical geometry. Instead, we calculate the single-particle real-space entanglement spectrum (EtS), which is an energy-like spectrum with virtual open boundary conditions [105–107]. By identifying gapless modes in EtS, we diagnose topological nature in each phase.

The EtS is determined from the properties of the correlation functions. We first review this using a quadratic BdG Hamiltonian as $(1/2) \sum_{ij} \mathbf{a}_i^\dagger H_{ij} \mathbf{a}_j$ with $\mathbf{a}_i^\dagger = (a_i^\dagger, a_i)$ on a lattice, where spin or orbital indices can be added along with the spatial coordinate i . By dividing the system into two parts, A and B , the entanglement Hamiltonian \mathcal{H}_A is defined by

$$\rho_A \equiv \text{tr}_B \rho = \frac{1}{Z} e^{-\mathcal{H}_A}, \quad (35)$$

where $\rho = |G\rangle \langle G|$ with $|G\rangle$ the ground state, tr_B refers to the trace over the region B , and Z is a normalization constant. The entanglement Hamiltonian also has a quadratic form as $\mathcal{H}_A = (1/2) \sum_{ij \in A} \mathbf{a}_i^\dagger (H_A)_{ij} \mathbf{a}_j$ [108]. The matrix H_A can be expressed using the correlation function matrix $(C_A)_{i,j \in A} = \text{tr} [\rho_A \mathbf{a}_i \mathbf{a}_j^\dagger]$ as [108–110]

$$C_A = \frac{1}{1 + e^{-H_A}}. \quad (36)$$

Since the spectra of H_A and C_A have the qualitatively same structure, we focus on C_A and refer to its eigenvalues ζ_k 's as the EtS below. The particle-hole symmetry $PH_A P^{-1} = -H_A$ leads to $PC_A P^{-1} = 1 - C_A$, where P is an anti-unitary matrix. Therefore, the EtS is symmetric with respect to $1/2$ because of $0 \leq \zeta_k \leq 1$.

Assuming the validity of applying the above discussion to a continuum system, we calculate the correlation function only on the northern hemisphere (NH) as

$$\begin{aligned} C_{\text{NH}}(\vec{\Omega}, \vec{\Omega}') &\equiv \int_{\text{NH}} d\vec{\Omega} \langle G | \mathbf{c}(\vec{\Omega}) \mathbf{c}^\dagger(\vec{\Omega}') | G \rangle \\ &= \delta(\vec{\Omega}, \vec{\Omega}') + Y(\vec{\Omega}) A Y^\dagger(\vec{\Omega}'), \end{aligned} \quad (37)$$

where $\mathbf{c}^\dagger = (c_\uparrow^\dagger, c_\downarrow^\dagger, c_\uparrow, c_\downarrow)$. The matrices in the second line in Eq. (37) are defined as follows:

$$\delta(\vec{\Omega}, \vec{\Omega}') \equiv \begin{pmatrix} \delta^2(\vec{\Omega} - \vec{\Omega}') & & & \\ & \delta^2(\vec{\Omega} - \vec{\Omega}') & & \\ & & 0 & \\ & & & 0 \end{pmatrix}, \quad (38)$$

$$Y = \begin{pmatrix} \mathbf{Y}_{Q_+Q_+} & & & \\ & \mathbf{Y}_{Q_-Q_+} & & \\ & & \mathbf{Y}_{Q_+Q_+}^* & \\ & & & \mathbf{Y}_{Q_-Q_+}^* \end{pmatrix} \quad (39)$$

$$A = \begin{pmatrix} -M_u M_u^\dagger & -M_u M_v^\dagger \\ M_u^* M_v^T & M_u^* M_u^T \end{pmatrix}, \quad (40)$$

where

$$\mathbf{Y}_{Ql}(\vec{\Omega}) = (Y_{Ql-l}(\vec{\Omega}), \dots, Y_{Qu}(\vec{\Omega})), \quad (41)$$

$$M_u = \vec{v}_{1-} \otimes u, \quad (42)$$

$$M_v = \vec{v}_{1-}^* \otimes v. \quad (43)$$

Here, \otimes refers to the tensor product. Note that (u, v) has been defined in Eq. (34) above.

The EtS ζ_k is given by the eigenvalue problem,

$$\int_{\text{NH}} d\vec{\Omega}' C(\vec{\Omega}, \vec{\Omega}') \vec{\psi}_k(\vec{\Omega}') = \zeta_k \vec{\psi}_k(\vec{\Omega}). \quad (44)$$

By expanding $\vec{\psi}_k(\vec{\Omega}) = Y(\vec{\Omega}) \vec{\alpha}_k$ and operating $\int d\vec{\Omega} Y^\dagger(\vec{\Omega})$ from the left, Eq. (44) reduces to

$$(\delta' - AB) \vec{\alpha}_k = \zeta_k \vec{\alpha}_k, \quad (45)$$

where

$$B = \int_{\text{NH}} d\vec{\Omega} \vec{Y}^\dagger \vec{Y}, \quad (46)$$

$$\delta' = \text{diag}\{\mathbf{1}_{4Q_++2}, \mathbf{0}_{4Q_++2}\}, \quad (47)$$

with $\mathbf{1}_n$ ($\mathbf{0}_n$) the n -dimensional identity (zero) matrices. Although $\delta' - AB$ is not hermitian, Eq. (45) can be transformed to an Hermitian problem as

$$(\delta' - B^{1/2} A B^{1/2}) \vec{\alpha}'_k = \zeta_k \vec{\alpha}'_k, \quad (48)$$

where $\vec{\alpha}'_k = B^{1/2} \vec{\alpha}_k$. We note that A is Hermitian, and $B = \text{diag}\{B_\uparrow, B_\downarrow, B_\uparrow, B_\downarrow\}$ with $(B_\sigma)_{mm'} = \delta_{mm'} \int_{\text{NH}} d\vec{\Omega} |Y_{Q_\pm Q_\pm m}|^2$ is positive-definite (This integration reduces to the Beta function). While one obtains $\zeta_k = 0$ or 1 at $\mu \rightarrow -\infty$, the ground state at $\mu \rightarrow \infty$, i.e. the IQH state, produces ‘‘entanglement gapless modes’’ that cross $\zeta_k = 0$ and 1 [111]. Below, we explore the EtS in the intermediate range of μ .

Figure 4(a) illustrates the EtS at $\Delta_0 = 4$ as a function of the chemical potential μ . In comparison, Fig. 4(b) shows the BdG spectrum, revealing two gap-closing points at $\mu \sim \pm 0.05$. The mid-gap states suddenly appear in the EtS at $\mu \sim -0.05$, and their density increases

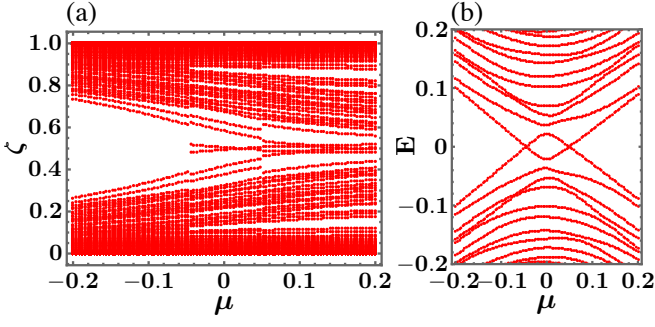


FIG. 4. (a) EtS and (b) BdG spectrum at $\Delta_0 = 4$ with $2Q = 222$. We set $\Gamma = 1$.

discretely at $\mu \sim 0.05$. This observation is consistent with the existence of the three phases, namely, the trivial ($C = 0$), the topological superconducting ($C = 1/2$), and the IQH ($C = 1$) phases. In the figures, we set $2Q = 222$ because this system has the relatively large energy gap of the ground state, resulting in less finite-size effect in the EtS.

C. Ensemble average

So far we have discussed findings based on a single impurity distribution. In the remainder of the work, we will present results using multiple random distributions.

Figure 5(a) is an analog of Fig. 3(d) but incorporates 300 random distributions of impurities. This is a 2D histogram where the gray color represents the normalized count of local-minimum-gap samples at each point. The superconducting phase is expected to emerge in $\Delta_{1c} < \Delta_0 < \Delta_{2c}$ and $\mu_L < \mu < \mu_R$ as indicated by a star. Each phase boundary is identified as follows: Figure 5(b) plots the probability of having M local-minimum gap points, denoted P_M , as a function of Δ_0 . We define Δ_{c1} (Δ_{c2}) by intersections of $P_{M \geq 3}$ and $P_{M=2}$ ($P_{M=2}$ and $P_{M=1}$). We determine μ_R and μ_L using histograms as in Fig. 5(c), where the green (orange) bars represent the distribution of left (right) local-minimum gap points. We define μ_L and μ_R as means for each dataset.

To explore the thermodynamic limit, we calculate Δ_{c1} and Δ_{c2} for different $2Q$'s in the above way, and present the results in Fig. 6. The dashed lines indicate the mean values of each dataset. The difference $\Delta_{c2} - \Delta_{c1}$ appears to remain finite as systems increase in size, suggesting the presence of the topological superconducting phase in the thermodynamic limit. We have chosen $2Q = 198$ in the above analysis as a representative example because it is the largest $2Q$ within the five closest systems to the two dashed lines.

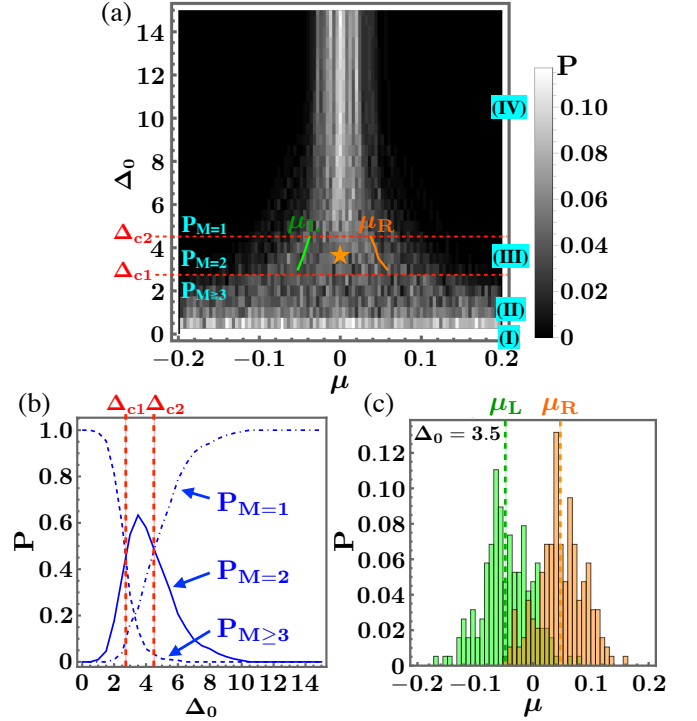


FIG. 5. (a) Distribution of local-minimum gap points. The color indicates the normalized count. The star denotes the topological superconducting regime, enclosed by two red-dashed lines (representing Δ_{c1} and Δ_{c2}) and green and orange line (representing μ_L and μ_R). (b) Probability of having M local-minimum gap points. The values of Δ_{c1} and Δ_{c2} are deduced from intersections of each line. (c) Distribution of local-minimum gap points with $M = 2$ at $\Delta_0 = 3.5$. The green and orange colors represent data for the left and right local-minimum gap, respectively. The values of μ_L and μ_R are defined as means for each dataset. We set $2Q = 198$ and $\Gamma = 1$ in all of the figures.

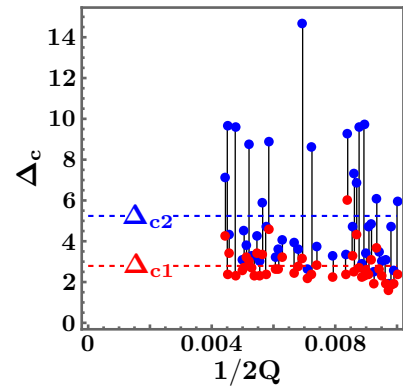


FIG. 6. Size-scaling analysis for Δ_{c1} (red dots) and Δ_{c2} (blue dots). The black lines connect the red and the blue dots at each $2Q$. The dashed lines represent the average of each dataset.

V. CONCLUDING REMARKS

In this paper, we formulate a scheme to combine the Rashba-coupled QH system with a type-II *s*-wave SC on the spherical geometry. Through this setup, we numerically demonstrate the emergence of a disorder-induced phase between a trivial and the IQH phases. We expect this to be the superconducting phase associated with the half-integer Chern number. This expectation is further supported by revealing the entanglement gapless modes in the EtS.

Our spherical model will be a useful platform for future study on topological order. Although we have focused on the (Rashba-coupled) IQH system, our formulation is also valid for the FQH system. The interplay between fractionalization and superconductivity can give rise to

intriguing phenomena such as \mathbb{Z}_n parafermions or Fibonacci anyons as mentioned in the introduction. The topological degeneracy of such states, stemming from their non-Abelian nature, is generally not exact in a finite system, which can lead to subtle problems in, for example, assessing degeneracy or energy excitations in a translationally invariant system. Our spherical model inherently avoids this issue, facilitating the straightforward identification of non-Abelian topological order.

ACKNOWLEDGMENTS

We acknowledge the computational resources offered by Research Institute for Information Technology, Kyushu University. The work is supported in part by JSPS KAKENHI Grant no. JP23K19036, JP20H01830, and JST CREST Grant no. JPMJCR18T2.

-
- [1] Y.-S. Wu, Phys. Rev. Lett. **52**, 2103 (1984), URL <https://link.aps.org/doi/10.1103/PhysRevLett.52.2103>.
- [2] F. Wilczek, Phys. Rev. Lett. **49**, 957 (1982), URL <http://link.aps.org/doi/10.1103/PhysRevLett.49.957>.
- [3] X.-G. Wen, Advances in Physics **44**, 405 (1995), <http://www.tandfonline.com/doi/pdf/10.1080/00018739500101566> URL <http://www.tandfonline.com/doi/abs/10.1080/00018739500101566>.
- [4] D. C. Tsui, H. L. Stormer, and A. C. Gossard, Phys. Rev. Lett. **48**, 1559 (1982), URL <http://link.aps.org/doi/10.1103/PhysRevLett.48.1559>.
- [5] R. B. Laughlin, Phys. Rev. Lett. **50**, 1395 (1983), URL <http://link.aps.org/doi/10.1103/PhysRevLett.50.1395>.
- [6] J. K. Jain, *Composite Fermions* (Cambridge University Press, New York, US, 2007).
- [7] V. Kalmeyer and R. B. Laughlin, Phys. Rev. Lett. **59**, 2095 (1987), URL <https://link.aps.org/doi/10.1103/PhysRevLett.59.2095>.
- [8] M. A. Levin and X.-G. Wen, Phys. Rev. B **71**, 045110 (2005), URL <http://link.aps.org/doi/10.1103/PhysRevB.71.045110>.
- [9] A. Kitaev, Annals of Physics **321**, 2 (2006), ISSN 0003-4916, january Special Issue, URL <http://www.sciencedirect.com/science/article/pii/S0003491605002381>.
- [10] G. Jackeli and G. Khaliullin, Phys. Rev. Lett. **102**, 017205 (2009), URL <https://link.aps.org/doi/10.1103/PhysRevLett.102.017205>.
- [11] N. Read and D. Green, Phys. Rev. B **61**, 10267 (2000), URL <http://link.aps.org/doi/10.1103/PhysRevB.61.10267>.
- [12] D. A. Ivanov, Phys. Rev. Lett. **86**, 268 (2001), URL <http://link.aps.org/doi/10.1103/PhysRevLett.86.268>.
- [13] Y. Kasahara, T. Ohnishi, Y. Mizukami, O. Tanaka, S. Ma, K. Sugii, N. Kurita, H. Tanaka, J. Nasu, Y. Motome, et al., Nature **559**, 227 (2018), URL <https://doi.org/10.1038/s41586-018-0274-0>.
- [14] T. Yokoi, S. Ma, Y. Kasahara, S. Kasahara, T. Shibauchi, N. Kurita, H. Tanaka, J. Nasu, Y. Motome, C. Hickey, et al., Science **373**, 568 (2021), <https://www.science.org/doi/pdf/10.1126/science.aay5551>, URL <https://www.science.org/doi/abs/10.1126/science.aay5551>.
- [15] J. A. N. Bruin, R. R. Claus, Y. Matsumoto, N. Kurita, H. Tanaka, and H. Takagi, Nature Physics **18**, 401 (2022), URL <https://doi.org/10.1038/s41567-021-01501-y>.
- [16] J. Nakamura, S. Liang, G. C. Gardner, and M. J. Manfra, Nature Physics **16**, 931 (2020), URL <https://doi.org/10.1038/s41567-020-1019-1>.
- [17] H. Bartolomei, M. Kumar, R. Bisognin, A. Marguerite, J.-M. Berroir, E. Bocquillon, B. Plaças, A. Cavanna, Q. Dong, U. Gennser, et al., Science **368**, 173 (2020), <https://www.science.org/doi/pdf/10.1126/science.aaz5601>, URL <https://www.science.org/doi/abs/10.1126/science.aaz5601>.
- [18] J. Nakamura, S. Liang, G. C. Gardner, and M. J. Manfra, *Fabry-perot interferometry at the $\nu = 2/5$ fractional quantum hall* (2023), 2304.12415.
- [19] A. Kitaev, Annals of Physics **303**, 2 (2003), ISSN 0003-4916, URL <http://www.sciencedirect.com/science/article/pii/S0003491602000180>.
- [20] C. Nayak, S. H. Simon, A. Stern, M. Freedman, and S. Das Sarma, Rev. Mod. Phys. **80**, 1083 (2008), URL <http://link.aps.org/doi/10.1103/RevModPhys.80.1083>.
- [21] J. K. Jain, Current Science **119**, 430 (2020).
- [22] L. Fu and C. L. Kane, Phys. Rev. Lett. **100**, 096407 (2008), URL <https://link.aps.org/doi/10.1103/PhysRevLett.100.096407>.
- [23] A. R. Akhmerov, J. Nilsson, and C. W. J. Beenakker, Phys. Rev. Lett. **102**, 216404 (2009), URL <https://link.aps.org/doi/10.1103/PhysRevLett.102.216404>.

- [24] J. D. Sau, R. M. Lutchyn, S. Tewari, and S. Das Sarma, Phys. Rev. Lett. **104**, 040502 (2010), URL <https://link.aps.org/doi/10.1103/PhysRevLett.104.040502>.
- [25] R. M. Lutchyn, J. D. Sau, and S. Das Sarma, Phys. Rev. Lett. **105**, 077001 (2010), URL <https://link.aps.org/doi/10.1103/PhysRevLett.105.077001>.
- [26] Y. Oreg, G. Refael, and F. Von Oppen, Physical review letters **105**, 177002 (2010).
- [27] J. Alicea, Phys. Rev. B **81**, 125318 (2010), URL <https://link.aps.org/doi/10.1103/PhysRevB.81.125318>.
- [28] X.-L. Qi, T. L. Hughes, and S.-C. Zhang, Phys. Rev. B **82**, 184516 (2010), URL <https://link.aps.org/doi/10.1103/PhysRevB.82.184516>.
- [29] B. Zocher and B. Rosenow, Phys. Rev. B **93**, 214504 (2016), URL <https://link.aps.org/doi/10.1103/PhysRevB.93.214504>.
- [30] R. V. Mishmash, A. Yazdani, and M. P. Zaletel, Phys. Rev. B **99**, 115427 (2019), URL <https://link.aps.org/doi/10.1103/PhysRevB.99.115427>.
- [31] G. Chaudhary and A. H. MacDonald, Phys. Rev. B **101**, 024516 (2020), URL <https://link.aps.org/doi/10.1103/PhysRevB.101.024516>.
- [32] M. Cheng, Physical Review B **86**, 195126 (2012).
- [33] N. H. Lindner, E. Berg, G. Refael, and A. Stern, Physical Review X **2**, 041002 (2012).
- [34] M. Burrello, B. van Heck, and E. Cobanera, Phys. Rev. B **87**, 195422 (2013), URL <https://link.aps.org/doi/10.1103/PhysRevB.87.195422>.
- [35] D. J. Clarke, J. Alicea, and K. Shtengel, Nature communications **4**, 1348 (2013).
- [36] A. Vaezi, Phys. Rev. B **87**, 035132 (2013), URL <https://link.aps.org/doi/10.1103/PhysRevB.87.035132>.
- [37] A. Milsted, E. Cobanera, M. Burrello, and G. Ortiz, Phys. Rev. B **90**, 195101 (2014), URL <https://link.aps.org/doi/10.1103/PhysRevB.90.195101>.
- [38] J. Klinovaja, A. Yacoby, and D. Loss, Phys. Rev. B **90**, 155447 (2014), URL <https://link.aps.org/doi/10.1103/PhysRevB.90.155447>.
- [39] J. Alicea and P. Fendley, Annual Review of Condensed Matter Physics **7**, 119 (2016), URL <https://doi.org/10.1146/annurev-commatphys-031115-011336>.
- [40] E. Sagi, A. Haim, E. Berg, F. von Oppen, and Y. Oreg, Phys. Rev. B **96**, 235144 (2017), URL <https://link.aps.org/doi/10.1103/PhysRevB.96.235144>.
- [41] J. Liang, G. Simion, and Y. Lyanda-Geller, Phys. Rev. B **100**, 075155 (2019), URL <https://link.aps.org/doi/10.1103/PhysRevB.100.075155>.
- [42] A. Vaezi, Phys. Rev. X **4**, 031009 (2014), URL <https://link.aps.org/doi/10.1103/PhysRevX.4.031009>.
- [43] R. S. K. Mong, M. P. Zaletel, F. Pollmann, and Z. Papić, Phys. Rev. B **95**, 115136 (2017), URL <http://link.aps.org/doi/10.1103/PhysRevB.95.115136>.
- [44] Y. Hu and C. L. Kane, Phys. Rev. Lett. **120**, 066801 (2018), URL <https://link.aps.org/doi/10.1103/PhysRevLett.120.066801>.
- [45] P. L. S. Lopes, V. L. Quito, B. Han, and J. C. Y. Teo, Phys. Rev. B **100**, 085116 (2019), URL <https://link.aps.org/doi/10.1103/PhysRevB.100.085116>.
- [46] O. Gül, Y. Ronen, S. Y. Lee, H. Shapourian, J. Zauberman, Y. H. Lee, K. Watanabe, T. Taniguchi, A. Vishwanath, A. Yacoby, et al., Phys. Rev. X **12**, 021057 (2022), URL <https://link.aps.org/doi/10.1103/PhysRevX.12.021057>.
- [47] Z. Tešanović, M. Rasolt, and L. Xing, Phys. Rev. Lett. **63**, 2425 (1989), URL <https://link.aps.org/doi/10.1103/PhysRevLett.63.2425>.
- [48] A. K. Rajagopal and R. Vasudevan, Phys. Rev. B **44**, 2807 (1991), URL <https://link.aps.org/doi/10.1103/PhysRevB.44.2807>.
- [49] Z. Tešanović, M. Rasolt, and L. Xing, Phys. Rev. B **43**, 288 (1991), URL <https://link.aps.org/doi/10.1103/PhysRevB.43.288>.
- [50] M. R. Norman, Phys. Rev. Lett. **66**, 842 (1991), URL <https://link.aps.org/doi/10.1103/PhysRevLett.66.842>.
- [51] H. Aker, A. H. MacDonald, S. M. Girvin, and M. R. Norman, Phys. Rev. Lett. **67**, 2375 (1991), URL <https://link.aps.org/doi/10.1103/PhysRevLett.67.2375>.
- [52] A. K. Rajagopal and J. C. Ryan, Phys. Rev. B **44**, 10280 (1991), URL <https://link.aps.org/doi/10.1103/PhysRevB.44.10280>.
- [53] M. Rasolt and Z. Tešanović, Rev. Mod. Phys. **64**, 709 (1992), URL <https://link.aps.org/doi/10.1103/RevModPhys.64.709>.
- [54] A. H. MacDonald, H. Aker, and M. R. Norman, Phys. Rev. B **45**, 10147 (1992), URL <https://link.aps.org/doi/10.1103/PhysRevB.45.10147>.
- [55] M. Norman, H. Aker, and A. MacDonald, Physica C: Superconductivity **196**, 43 (1992), ISSN 0921-4534, URL <https://www.sciencedirect.com/science/article/pii/092145349290135Y>.
- [56] A. K. Rajagopal, Phys. Rev. B **46**, 1224 (1992), URL <https://link.aps.org/doi/10.1103/PhysRevB.46.1224>.
- [57] A. MacDonald, H. Aker, and M. Norman, Australian Journal of Physics **46**, 333 (1993), URL <https://doi.org/10.1071/PH930333>.
- [58] J. Ryan and A. Rajagopal, Journal of Physics and Chemistry of Solids **54**, 1281 (1993), ISSN 0022-3697, special Issue Spectroscopies in Novel Superconductors, URL <https://www.sciencedirect.com/science/article/pii/002236979390180Y>.
- [59] J. C. Ryan and A. K. Rajagopal, Phys. Rev. B **47**, 8843 (1993), URL <https://link.aps.org/doi/10.1103/PhysRevB.47.8843>.
- [60] M. R. Norman, A. H. MacDonald, and H. Aker, Phys. Rev. B **51**, 5927 (1995), URL <https://link.aps.org/doi/10.1103/PhysRevB.51.5927>.
- [61] M. M. Maška, Phys. Rev. B **66**, 054533 (2002), URL <https://link.aps.org/doi/10.1103/PhysRevB.66.054533>.
- [62] P. Scherpelz, D. Wulin, B. c. v. Šopík, K. Levin, and A. K. Rajagopal, Phys. Rev. B **87**, 024516 (2013), URL <https://link.aps.org/doi/10.1103/PhysRevB.87.024516>.
- [63] S. Ran, I.-L. Liu, Y. S. Eo, D. J. Campbell, P. M. Neves, W. T. Fuhrman, S. R. Saha, C. Eckberg, H. Kim, D. Graf, et al., Nature Physics **15**, 1250 (2019), URL <https://doi.org/10.1038/s41567-019-0670-x>.
- [64] Y. Kim, A. C. Balram, T. Taniguchi, K. Watanabe, J. K. Jain, and J. H. Smet, Nature Physics **15**, 154 (2019), ISSN 1745-2481, URL <https://doi.org/10.1038/s41567-018-0355-x>.
- [65] G. Chaudhary, A. H. MacDonald, and M. R. Norman, Phys. Rev. Res. **3**, 033260 (2021), URL <https://link.aps.org/doi/10.1103/PhysRevResearch.3.033260>.
- [66] J. Schirmer, C.-X. Liu, and J. K. Jain,

- Proceedings of the National Academy of Sciences **119**, e2202948119 (2022), <https://www.pnas.org/doi/pdf/10.1073/pnas.2202948119>, URL <https://www.pnas.org/doi/abs/10.1073/pnas.2202948119>.
- [67] J. Schirmer, J. K. Jain, and C. X. Liu (2022), URL <https://arxiv.org/abs/2211.15001>.
- [68] X. G. Wen, Phys. Rev. Lett. **64**, 2206 (1990), URL <http://link.aps.org/doi/10.1103/PhysRevLett.64.2206>.
- [69] Y. Hatsugai, P.-A. Bares, and X. G. Wen, Phys. Rev. Lett. **71**, 424 (1993), URL <http://link.aps.org/doi/10.1103/PhysRevLett.71.424>.
- [70] J. S. Birman, Communications on Pure and Applied Mathematics **22**, 41 (1969), <https://onlinelibrary.wiley.com/doi/pdf/10.1002/cpa.3160220104>, URL <https://onlinelibrary.wiley.com/doi/abs/10.1002/cpa.3160220104>.
- [71] T. Einarsson, Phys. Rev. Lett. **64**, 1995 (1990), URL <https://link.aps.org/doi/10.1103/PhysRevLett.64.1995>.
- [72] X. G. Wen, Phys. Rev. B **41**, 12838 (1990), URL <http://link.aps.org/doi/10.1103/PhysRevB.41.12838>.
- [73] M. Oshikawa and T. Senthil, Phys. Rev. Lett. **96**, 060601 (2006), URL <https://link.aps.org/doi/10.1103/PhysRevLett.96.060601>.
- [74] M. Sato, M. Kohmoto, and Y.-S. Wu, Phys. Rev. Lett. **97**, 010601 (2006), URL <https://link.aps.org/doi/10.1103/PhysRevLett.97.010601>.
- [75] M. Oshikawa, Y. B. Kim, K. Shtengel, C. Nayak, and S. Tewari, Annals of Physics **322**, 1477 (2007), ISSN 0003-4916, URL <http://www.sciencedirect.com/science/article/pii/S0003491606001837>.
- [76] F. D. M. Haldane, Phys. Rev. Lett. **55**, 2095 (1985), URL <http://link.aps.org/doi/10.1103/PhysRevLett.55.2095>.
- [77] X. G. Wen and Q. Niu, Phys. Rev. B **41**, 9377 (1990), URL <https://link.aps.org/doi/10.1103/PhysRevB.41.9377>.
- [78] F. D. M. Haldane, Phys. Rev. Lett. **51**, 605 (1983), URL <http://link.aps.org/doi/10.1103/PhysRevLett.51.605>.
- [79] E. Rashba, Sov. Phys.-Solid State **2**, 1109 (1960).
- [80] Y. A. Bychkov and E. I. Rashba, Journal of Physics C: Solid State Physics **17**, 6039 (1984), URL <https://dx.doi.org/10.1088/0022-3719/17/33/015>.
- [81] J. Schliemann, J. C. Egues, and D. Loss, Phys. Rev. B **67**, 085302 (2003), URL <https://link.aps.org/doi/10.1103/PhysRevB.67.085302>.
- [82] S.-Q. Shen, M. Ma, X. C. Xie, and F. C. Zhang, Phys. Rev. Lett. **92**, 256603 (2004), URL <https://link.aps.org/doi/10.1103/PhysRevLett.92.256603>.
- [83] T. Ito, K. Nomura, and N. Shibata, Journal of the Physical Society of Japan **81**, 034713 (2012), <https://doi.org/10.1143/JPSJ.81.034713>, URL <https://doi.org/10.1143/JPSJ.81.034713>.
- [84] A. H. Castro Neto, F. Guinea, N. M. R. Peres, K. S. Novoselov, and A. K. Geim, Rev. Mod. Phys. **81**, 109 (2009), URL <http://link.aps.org/doi/10.1103/RevModPhys.81.109>.
- [85] T. T. Wu and C. N. Yang, Nucl. Phys. B **107**, 365 (1976).
- [86] T. T. Wu and C. N. Yang, Phys. Rev. D **16**, 1018 (1977), URL <http://link.aps.org/doi/10.1103/PhysRevD.16.1018>.
- [87] K. Nomura and A. H. MacDonald, Phys. Rev. Lett. **96**, 256602 (2006), URL <http://link.aps.org/doi/10.1103/PhysRevLett.96.256602>.
- [88] M. O. Goerbig, R. Moessner, and B. Douçot, Phys. Rev. B **74**, 161407 (2006), URL <http://link.aps.org/doi/10.1103/PhysRevB.74.161407>.
- [89] V. M. Apalkov and T. Chakraborty, Phys. Rev. Lett. **97**, 126801 (2006), URL <http://link.aps.org/doi/10.1103/PhysRevLett.97.126801>.
- [90] C. Tóke, P. E. Lammert, V. H. Crespi, and J. K. Jain, Phys. Rev. B **74**, 235417 (2006), URL <http://link.aps.org/doi/10.1103/PhysRevB.74.235417>.
- [91] C. Tóke and J. K. Jain, Phys. Rev. B **75**, 245440 (2007), URL <http://link.aps.org/doi/10.1103/PhysRevB.75.245440>.
- [92] A. C. Balram, C. Tóke, A. Wójs, and J. K. Jain, Phys. Rev. B **92**, 205120 (2015), URL <http://link.aps.org/doi/10.1103/PhysRevB.92.205120>.
- [93] A. Jellal, Nucl. Phys. B **804**, 361 (2008), ISSN 0550-3213, URL <http://www.sciencedirect.com/science/article/pii/S0550321308002307>.
- [94] M. Arciniaga and M. R. Peterson, Phys. Rev. B **94**, 035105 (2016), URL <http://link.aps.org/doi/10.1103/PhysRevB.94.035105>.
- [95] K. Hasebe, International Journal of Modern Physics A **31**, 1650117 (2016), <http://www.worldscientific.com/doi/pdf/10.1142/S0217751X16501177>, URL <http://www.worldscientific.com/doi/abs/10.1142/S0217751X16501177>.
- [96] K. Yonaga, K. Hasebe, and N. Shibata, Phys. Rev. B **93**, 235122 (2016), URL <http://link.aps.org/doi/10.1103/PhysRevB.93.235122>.
- [97] M. J. W. Dodgson, Journal of Physics A: Mathematical and General **29**, 2499 (1996), URL <https://dx.doi.org/10.1088/0305-4470/29/10/028>.
- [98] M. J. W. Dodgson and M. A. Moore, Phys. Rev. B **55**, 3816 (1997), URL <https://link.aps.org/doi/10.1103/PhysRevB.55.3816>.
- [99] W. H. Kleiner, L. M. Roth, and S. H. Autler, Phys. Rev. **133**, A1226 (1964), URL <https://link.aps.org/doi/10.1103/PhysRev.133.A1226>.
- [100] J. J. Thomson, Phil. Mag. **7**, 237 (1904).
- [101] D. J. Wales and S. Ulker, Phys. Rev. B **74**, 212101 (2006), URL <https://link.aps.org/doi/10.1103/PhysRevB.74.212101>.
- [102] D. J. Wales, H. McKay, and E. L. Altschuler, Phys. Rev. B **79**, 224115 (2009), URL <https://link.aps.org/doi/10.1103/PhysRevB.79.224115>.
- [103] J. Zhao, Y. Zhang, and J. K. Jain, Phys. Rev. Lett. **121**, 116802 (2018), URL <https://link.aps.org/doi/10.1103/PhysRevLett.121.116802>.
- [104] T. Ando, Journal of the Physical Society of Japan **52**, 1740 (1983), URL <https://doi.org/10.1143/JPSJ.52.1740>.
- [105] S. Ryu and Y. Hatsugai, Phys. Rev. B **73**, 245115 (2006), URL <https://link.aps.org/doi/10.1103/PhysRevB.73.245115>.
- [106] H. Li and F. D. M. Haldane, Phys. Rev. Lett. **101**, 010504 (2008), URL <http://link.aps.org/doi/10.1103/PhysRevLett.101.010504>.
- [107] E. Prodan, T. L. Hughes, and B. A. Bernevig, Phys. Rev. Lett. **105**, 115501 (2010), URL <https://link.aps.org/doi/10.1103/PhysRevLett.105.115501>.

- [108] I. Peschel, *Journal of Physics A: Mathematical and General* **36**, L205 (2003), URL <https://dx.doi.org/10.1088/0305-4470/36/14/101>.
- [109] S.-A. Cheong and C. L. Henley, *Phys. Rev. B* **69**, 075111 (2004), URL <https://link.aps.org/doi/10.1103/PhysRevB.69.075111>.
- [110] T. P. Oliveira, P. Ribeiro, and P. D. Sacramento, *Journal of Physics: Condensed Matter* **26**, 425702 (2014), URL <https://dx.doi.org/10.1088/0953-8984/26/42/425702>.
- [111] I. D. Rodríguez and G. Sierra, *Phys. Rev. B* **80**, 153303 (2009), URL <https://link.aps.org/doi/10.1103/PhysRevB.80.153303>.